Modelling Multilayer Communication Channel in Terahertz Band for Medical Applications

Essraa Hesham[1], Mohammed S. Gadelrab[2], Khaled ElSayed[1] and Abdel Rahman Sallam[2]

[1]Faculty of Engineering, Cairo University, Egypt
[2]National Institute of Standard, Egypt

***Abstract*:** In this work we present a multi-layer channel model for terahertz communication that incorporates both layers of human body tissues and textile layers. Many research works tackled communication channel modelling in human body alone while some other research focused on textile characterization/modelling alone. There is a real gap in connecting these different models. To investigate this, a multi-layer channel model for terahertz communication is developed, this model assumes external textile layer stacked over layers of human body tissues. The electromagnetic properties of the different layers are extracted from previous works that used time domain spectroscopy (TDS) in the terahertz band to characterize each of the considered layers. The model is implemented as a flexible MATLAB/Octave program that enables the simulation of layers with either fixed or random depths. This paper aims to pave the way to connecting patients' in-body nano-nodes with off-body (on-cloth) nano-nodes by building such a combined channel model. This helps in many applications especially in the medical field. For example, having connected nano-nodes can help in diagnosing diseases, monitoring health by sending information to the external environment, treatment (e.g., increasing or decreasing a certain dose depending on the monitoring), etc. The obtained results show how the THz signal can be affected when it propagates through heterogeneous mediums (i.e., human body tissues and textile). Various types of path-loss have been calculated for this purpose and verified by comparison with results from previous research on separate models of human body and textile.

***Keywords*:** Multi-layer, Channel modeling, Channel Characterization, path-loss, Terahertz frequency, Wireless Body Area Network (WBAN)**.**

1. Introduction

Often nano-communication through electromagnetic waves is carried out at the terahertz (THz) range from 0.1 to 10 THz. The THz frequency band has several advantages and applications [1] and [2]. For example, it is not currently allocated by regulatory bodies to any communication service, which allows using ultra-wide bandwidth communication schemes. This, in turn, supports high bit rates in the range of Terabits per second. Also, it is non-ionizing inside the body and not very susceptible to scattering effects.

Nano-communication have several medical applications such as diagnosis and monitoring patient health. The main goal of this research is to develop a communication channel model that can be suitable for studying these applications. Several research works have been already done on THz communication channels inside the human body such as [3] and [4]. Other researches have been conducted on THz textile characterization and THz textile antenna [5] and [6] where terahertz waves show promise in detecting and imaging objects under obscuring material [7]. Up to our knowledge no published work has been reported for a communication channel composed of both human body tissues and textile (body + textile).

In order to allow in-body nano-nodes to communicate with off-body (on-clothes) nano-nodes we need to characterize several layers of body tissues and textile. Then, we have to develop a model for that communication channel and analyze its various characteristics such as propagation, path-losses, noise, channel capacity, etc. We build our model based on analytical equations describing electromagnetic propagation in a dielectric medium where the electromagnetic properties of human tissues were collected from measurements provided in different sources [4] and [3]. First, we implement a multi-layered sub-model for the in-body part of the communication channel using *Octave* [8], which is an open-source equivalent of *MATLAB* [9]. The results of our model are compared with the results of similar previous work on THz communication channels in human body to verify the behavior of our model.

Then, we have developed another sub-model for a channel composed of air-cotton-air layers such that we can analyze its characteristics and compare the results with previous work on terahertz textile characterization.

Developing two sub-models is essential to verify the results to substitute for the lack of direct measurements. Finally, we integrate these two sub-models to construct the complete model for in-body-on-cloth communication channel. The resulting model enables us to analyze various properties of an electromagnetic signal traversing the human skin and the air-cotton-air model at terahertz frequencies.

This paper is organized as follows: Section 2 outlines our approach. Section 3 describes how we constructed our channel model. Section 4 presents the results, followed by a discussion and the conclusion in sections 5 and 6 respectively.

2. Multi-Layer Air-Cloth-Air-Human_body Terahertz Channel Modelling

Wireless body area networks (WBAN) in healthcare applications involve secure communication from inside the human body towards outside objects such as on-body wearable devices or smart clothes [19]. In this work, we tackle this problem at low level by developing two separate sub-models of the communication channel: one for the inside body part and the other for the off-body part (i.e., clothes). These two sub-models are then integrated to create the final model. We derived the equations that characterize all model layers as presented in this section. The resulting equations are confirmed to be in alignment with the previous work in [3].

2.1 Path-losses

The total path-loss depends on several factors including the molecular compositions, the transmission distances and the frequency. It consists mainly of the spreading loss, the

molecular absorption loss, and the scattering loss. The spreading loss corresponds to the attenuation when a wave propagates through the medium. The absorption loss is the attenuation due to the absorbed energy by molecules along the transmission path, which converts a part of wave energy into internal kinetic energy at the molecular level. Moreover, because of the presence of stratified medium stack, losses due to reflection in interface boundaries are added. The stratified medium stack is a stack of different thin films where the human skin has different layers (blood epidermis, hypodermis) each having different electromagnetic properties. This leads to the equation:

$$PL_{total} = PL_{spread} + PL_{absorb} + PL_{scatter} + PL_{ref} \quad (1)$$

where:
PL_{total}: is the total path-loss
PL_{spread}: is the spreading path-loss
PL_{absorb}: absorption path-loss
PL_{ref}: is the reflection path-loss

Scattering path-loss depends on the relative size of the material molecules and the wavelength of the electromagnetic wave. It can be omitted here because its effect is negligible compared to the other path-loss factors. Therefore, Eqn.1 can be simplified as follows:

$$PL_{total} = PL_{spread} + PL_{absorb} + PL_{ref} \quad (2)$$

The spreading path-loss can be expressed by the Friis transmission formula [10], which relates the free space path-loss, antenna gains and wavelength to the received and transmitted power:

$$PL_{spread} = D.\left(\frac{\lambda_g}{4\pi d}\right)^2 \quad (3)$$

where:
D: is the directivity of the transmitting antenna
d: is the distance the wave has traveled
λ_g: is the effective wavelength

$$\lambda_g = \lambda / n' \quad (4)$$

Where: n' is the real component of the refractive index n of the medium: $n = n' - n''$
The absorption path-loss or the attenuation due to the absorption of an electromagnetic wave passing through a dispersive medium can be calculated from Beer-Lambert law [11]:

$$PL_{absorb} = e^{-\mu_{absorb}.d} \quad (5)$$

where μ_{absorb}: is the attenuation coefficient due to absorption which is given as:

$$\mu_{absorb} = \frac{4\pi.n''}{\lambda} \quad (6)$$

The reflection losses at the interface boundaries can be calculated by using the Fresnel equations for non-magnetic medium since human tissues have no magnetic properties in the terahertz band.

$$PL_{ref} = \left(\frac{n'_1 - n'_2}{n'_1 + n'_2}\right)^2 \quad (7)$$

where n'_1 and n'_2 are the refractive indices of the medium that the wave is propagating from and to respectively.
The refractive index of the medium can be calculated as a function of the permittivity ϵ. It has different equations according to the nature of the medium of the layers. For example, for the in-body sub-model, we use the Havriliak–Negami [12] equation for one relaxation process in the epidermis layer, the Havriliak–Negami equation for two relaxation processes in the dermis and hypodermis, the double-Debye equation for two relaxation processes. Debye [13] and Havriliak–Negami equations are explained in the next sub-section. For the on-body sub-model, air permittivity is approximated as the permittivity of the free space [16]. The refractive index and the absorption coefficient of the cotton over the designated range (0.5-1.5 THz) are obtained from measurements and calculations in a previous work by Li *et al.* [5].
There is another method to calculate the reflection loss using the ABCD matrix [7], which is out of the scope of this paper due to space limitations. Meanwhile, it can be used to further compare and verify the results.

2.2 Dielectric Characteristics

Permittivity is an important parameter that measures the electric polarizability of a dielectric. The complex permittivity can be expressed as:

$$\epsilon_r = \epsilon'_r - i\epsilon''_r \quad (8)$$

The refractive index can be expressed in terms of relative permittivity and relative permeability μ_r as: $n = \sqrt{\epsilon_r \mu_r}$, both human and cotton tissues has no magnetic properties, thus the magnetic permeability μ_r can be approximated to one:

$$n \approx \sqrt{\epsilon_r} \quad (9)$$

The human tissue consists of nano structures mostly dominated by water molecules. Therefore, Debye equations would be applicable:

$$\epsilon_r = \epsilon_\infty + \sum_k \left(\frac{\triangle \epsilon_k}{1 + i\omega T_k}\right) \quad (10)$$

$$\epsilon'_r = \epsilon_\infty + \frac{\triangle \epsilon_k}{1 + (\omega T_k)^2} \quad (11)$$

$$\epsilon''_r = \frac{\triangle \epsilon_k (\omega T_k)}{1 + (\omega T_k)^2} \quad (12)$$

where:
k: signifies different relaxation processes,
ϵ_∞: is the permittivity at the high frequency limit,
ϵ_s: is the static permittivity at the low frequency limit,
T: is the characteristic relaxation time relating to that specific process,
ω: is the angular frequency
$\triangle \epsilon$: is the permittivity difference between each relaxation process for only one process:

$$\triangle \epsilon = \epsilon_s - \epsilon_\infty \quad (13)$$

Havriliak and Negami [12] take into account the asymmetry and broadness of the dielectric dispersion curve. The modified model calculates relative permittivity as:

$$\epsilon_r = \epsilon_\infty + \sum_k \frac{\triangle \epsilon_k}{(1 + (\omega T_k)^\alpha)^\beta} - j\frac{\sigma}{\omega \epsilon_o} \quad (14)$$

where:
σ: is the ionic static conductivity,
ϵ_o: is the free space permittivity that approximately equals: $8.854x10^{-12} Fm^{-1}$,

α and β are heuristically derived power law exponents [3].
The relative and imaginary components can be calculated as:

$$\epsilon'_r = \epsilon_\infty + \triangle \epsilon_k \left(1 + 2(\omega T_k)^\alpha cos\left(\frac{\pi\alpha}{2}\right) + (\omega T_k)^{2\alpha}\right)^{\frac{-\beta}{2}} cos(\beta \emptyset_k) \quad (15)$$

$$\epsilon''_r = \triangle \epsilon_k \left(1 + 2(\omega T_k)^\alpha cos\left(\frac{\pi\alpha}{2}\right) + (\omega T_k)^{2\alpha}\right)^{\frac{-\beta}{2}} sin(\beta \emptyset_k) - \frac{\sigma}{\omega \epsilon_o} \quad (16)$$

$$\emptyset_k = arctan\left(\frac{(\omega T_k)^{\alpha_k} sin\left(\frac{\pi\alpha_k}{2}\right)}{1+(\omega T_k)^{\alpha_k} cos\left(\frac{\pi\alpha_k}{2}\right)}\right) \quad (17)$$

2.3 The Proposed in-body and off-body Model

Figure 1 shows the first sub-model for the in-body part of the channel. The human skin is far more complex than what is considered here with all of the different constituents of skin such as hair follicles, glands, network of capillaries and even sweat ducts [14]. All have shown to have electrical properties affecting the propagation of electromagnetic waves. For simplicity, the superficial layers of the human body tissues, near the skin, are considered. The depicted model consists of four layers: epidermis, dermis, blood and hypodermis; ordered from outside to inside.
The second sub-model is shown in Figure 2. It represents the on-body part of the channel. This consists of three layers: air, cotton, and air. The two sub-models are constructed as an intermediate step to generate partial results for simplification and verification purposes.
The total path-loss is calculated for the entire channel model shown schematically in Figure 3. This model represents electromagnetic wave propagation through on-body or clothes layer and human body tissues. The thickness of each layer are assigned such that air-cotton-air lie between 1-2 mm, while for in-body layers, thickness values are aligned with Ref. [14].

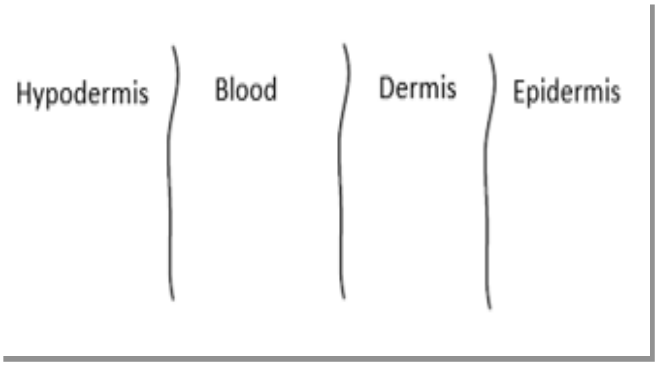

Figure 1. Structure of the in-body sub-model.

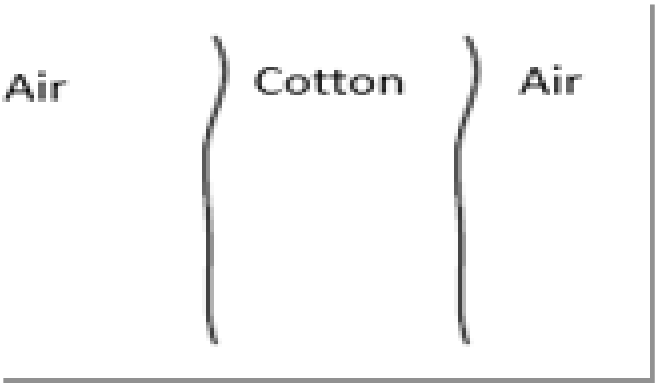

Figure 2. Structure of the on-body sub-model.

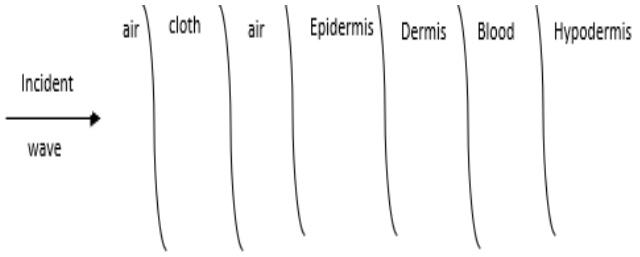

Figure 3. Structure of the complete model for the whole channel.

3. Results

3.1 In-body Sub-Model

This section presents the partial results of the in-body and the on-body separately. Overall, the partial results of our sub-models are closely comparable with the results of similar research such as] and Regarding the in-body sub-model, Figure 4 shows the spreading path-loss with boundary matching against distance from 0 to 7 mm at frequency ranges from 0.5 to 1.5 THz for the 4-layer human skin model. The spreading path-loss does not seem to be very material dependent with respect to human body tissues. In fact, it only differs by few dB when compared with different materials side by side over the whole distance. Our results agree with the results in which is easily noticeable and well-expected since the layers of our in-body model are identical to theirs.

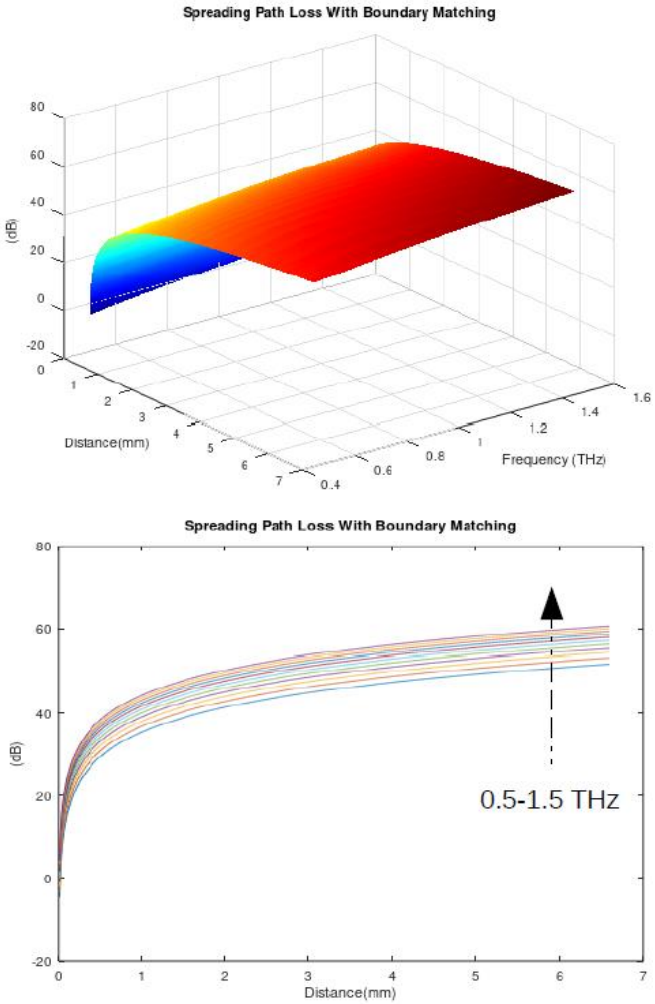

Figure 4. 3D & 2D spreading PL for in-body sub-model.

Figure 5 shows the absorption path-loss with boundary matching against distance from 0 to 7mm at frequencies from 0.5 to 1.5 THz. We noticed that the absorption path-loss is higher than that of the spreading path-loss where we can observe clear differences between the different tissues. We can also see that the signal seems to suffer from the highest amount of attenuation through the blood layer. Results show agreement with published results of [3], where absorption path-loss is the largest in blood layer. The general behavior of the skin and fat curves in [4] is closely comparable to the obtained results of our model.

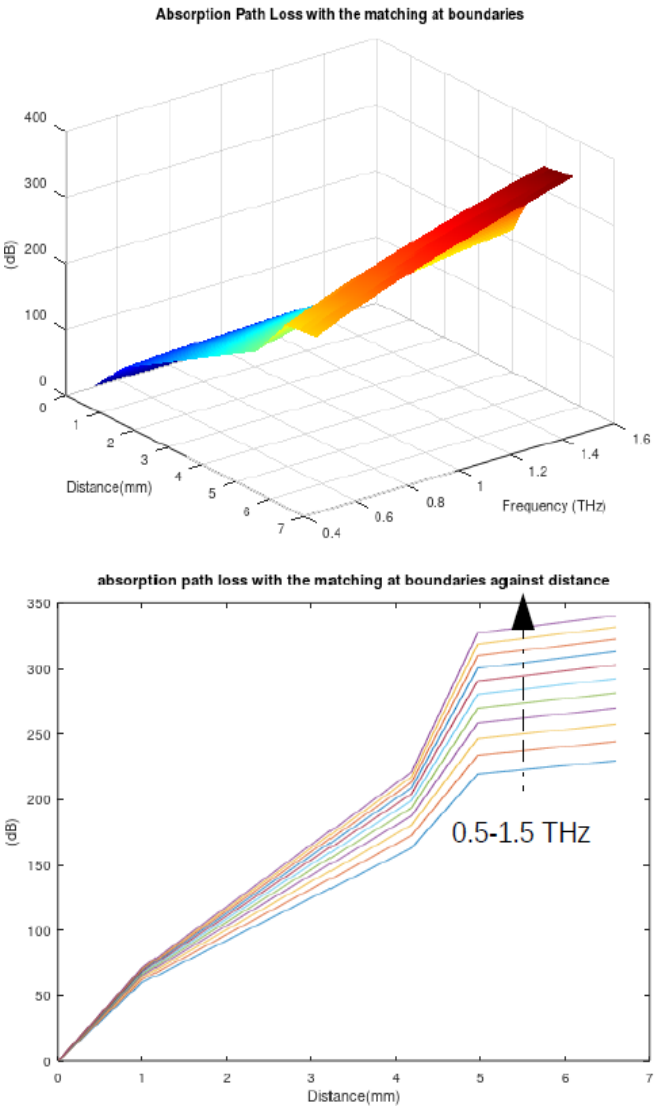

Figure 5. 3D & 2D absorption PL for in-body sub-model.

Figure 6 shows the total path-loss against both frequency and distance for the 4-layer human skin model. We can observe that the total path-loss for an electromagnetic signal travelling through a randomized human tissue stack of depth 6.58 mm seems to suffer between 300-375 dB for the frequency range 0.5-1.5 THz, which complies too with the results in [3] and

The absorption coefficient, reflection and permittivity are important parameters in our equations to calculate path-losses (see eqn. (2)).

Figure 7 plots the calculated frequency-dependent absorption coefficient of the four layers in the human body tissue model. Figure 8 plots the frequency-dependent reflection displayed in % for the three different interfaces of our four layered human body tissue model. The reflection for these specific boundaries reached a maximum of 1.6% which amounts to a loss of less than 0.1 db. Figure 9 displays the imaginary and the real parts of the permittivity of the different layers of the in-body model. The results reproduces and confirms the results obtained in [2] and [4].

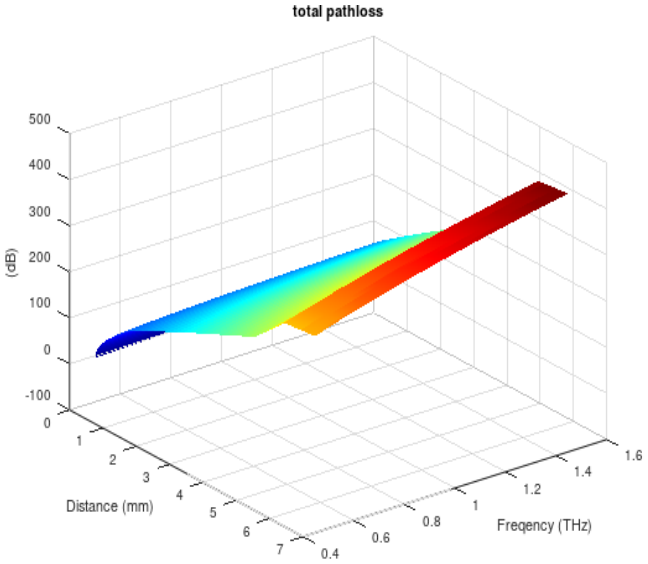

Figure 6. Total path-loss against for in-body sub-model.

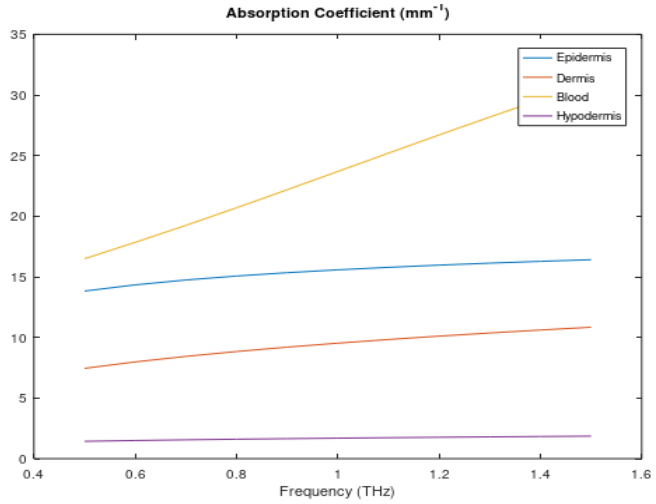

Figure 7. Absorption coefficient for in-body sub-model.

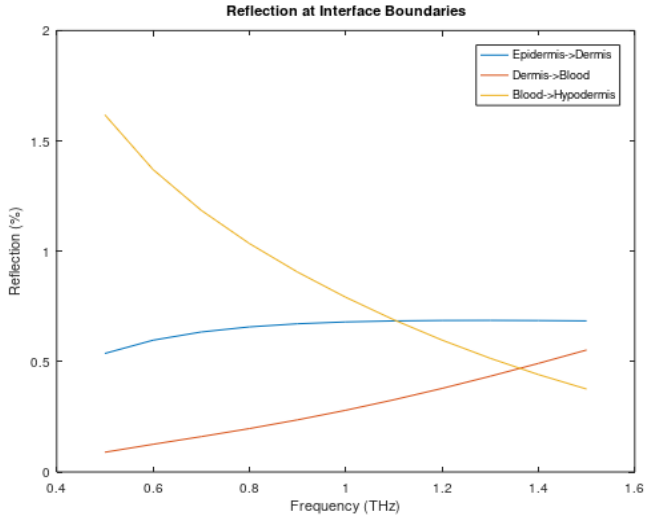

Figure 8. Reflection at interference boundary for in-body sub-model.

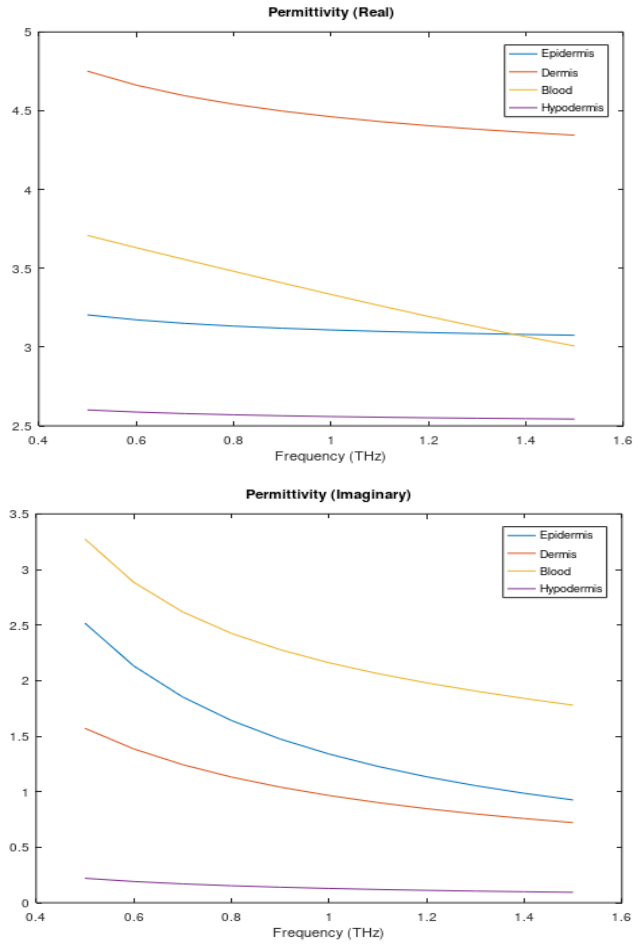

Figure 9. Real & imag. parts of human body tissue permittivity.

3.2 On-body Sub-Model

Regarding the on-body sub-model, the spreading path-loss and the absorption path-loss are shown in Figure 10 and Figure 11, respectively. The distance ranges from 0 to 4mm (1mm air, 2mm cotton and 1mm air) at frequencies from 0.5 to1.5. The significant loss occurs when the signal traverses the cotton layer where it suffers from the highest amount of attenuation, which is expected when compared to the loss in the air layers (almost 0). This situation represents ideal conditions of dry air. However, in practice the humidity, the temperature and the presence of water vapor particles would certainly affect the losses in the air layers.

Figure 12 shows the total path-loss against both frequency and distance for the three layers: air, cotton, air. We can observe that the total path-loss for an electromagnetic signal traveling through a randomized depth 4 mm seems to suffer between 0-70 dB for the frequency range 0.5-1.5 THz.

The spectral characteristics of cotton in the range of 0.5～1.5 THz have been measured with THz time domain spectroscopy. It is found that cotton has the spectral response to THz waves in this frequency region, eqn. (2) from [5] is used to calculate the refractive index of cotton instead of measuring due to the lack of such devices as Terahertz Time Domain Spectroscopy (TDS), the refractive index is very important in the calculation of the losses, the spectral response are obtained at room temperature in nitrogen atmosphere [5].

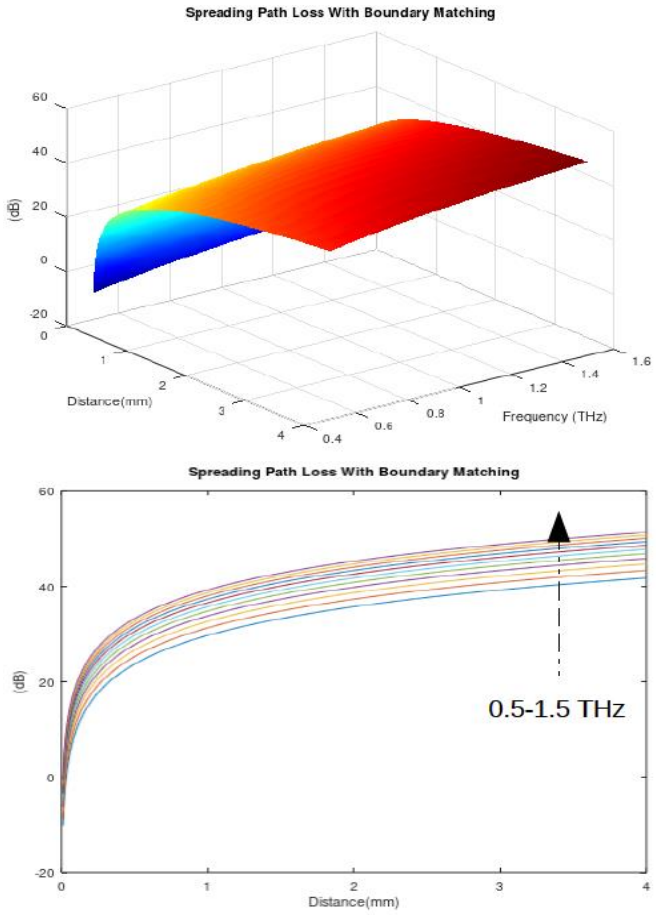

Figure 10. 3D & 2D spreading path-loss with boundary matching for on-body sub-model.

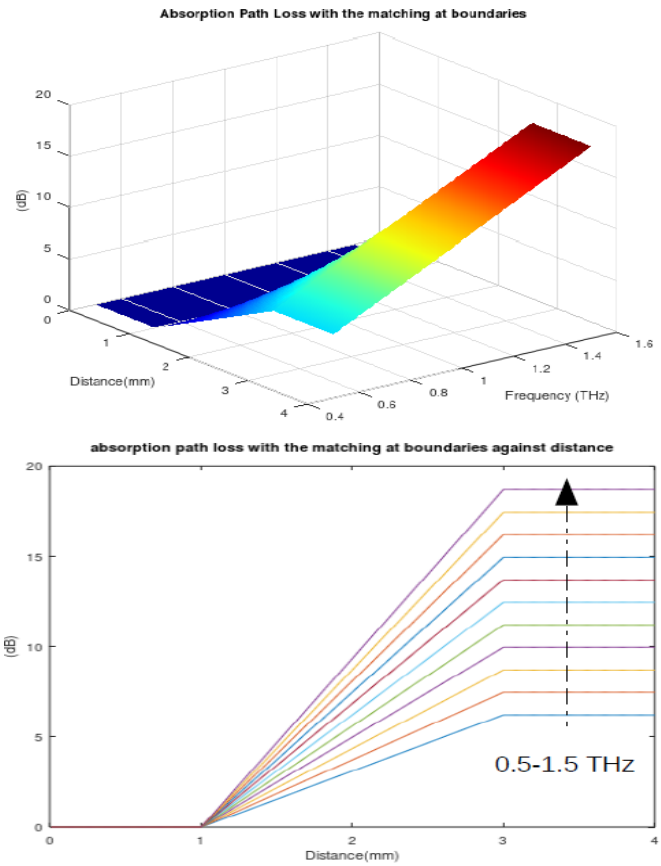

Figure 11. 3D & 2D absorption path-loss with boundary matching for the on-body sub-model.

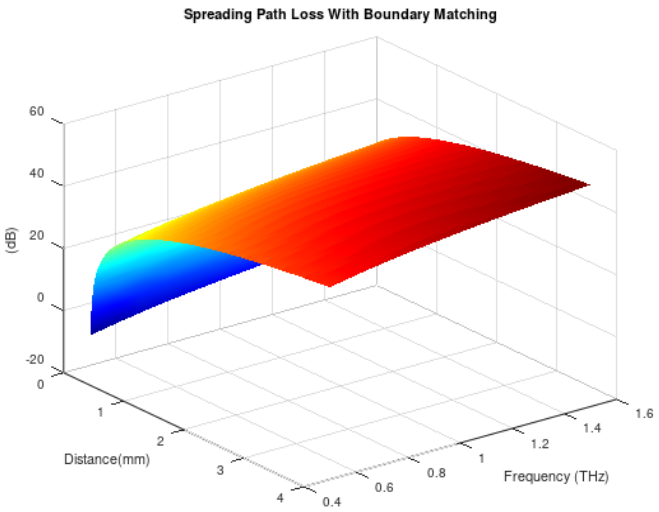

Figure 12. The total path-loss for the on-body sub-model.

3.3 Entire Channel Model

The previous results are only intermediate results for verification purposes. Our final goal is to study losses in the entire channel that consists of human body tissues and cotton layer, which is presented by the remaining figures. We follow the same sequence by presenting the spreading loss, the absorption loss and the total loss for the entire channel. Figure 13 illustrates the spreading path-loss with boundary matching against distance from 0 to 12mm and frequency ranging from 0.5 to 1.5 THz for the entire communication channel (i.e., both the 4-layer human tissues and on-body 3 layers).

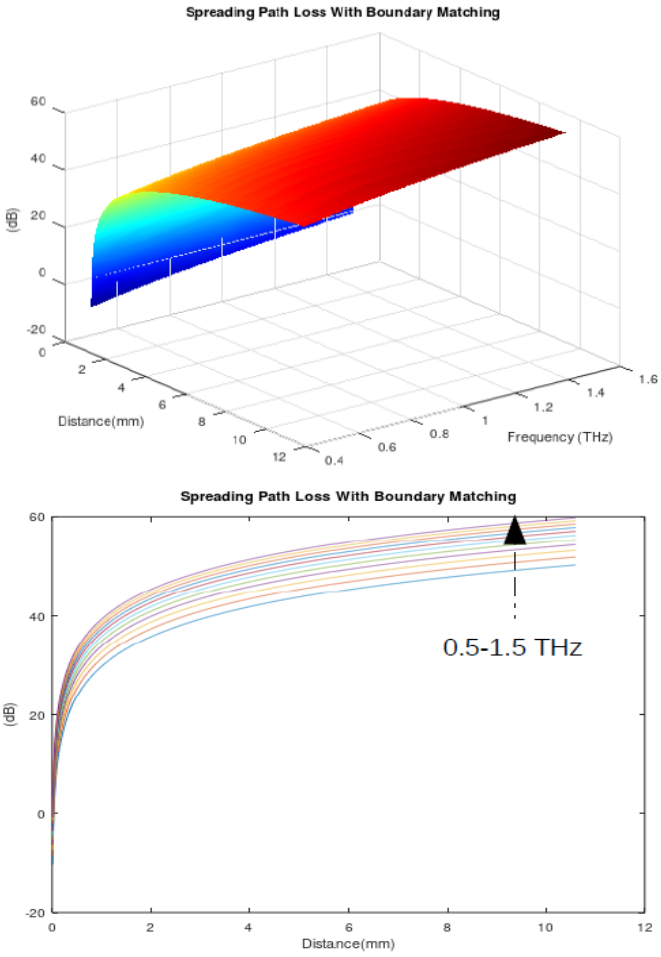

Figure 13. 3D and 2D spreading path-loss with boundary matching for the entire channel.

Similarly, Figure 14 shows the absorption path-loss with boundary matching against distance from 0 to 12mm and frequency ranging from 0.5-1.5 THz. The absorption path-loss is much higher than that of spreading and we see clear differences between the different tissues and layers. Figure 15 shows the absorption coefficient of the seven layers of the entire channel (i.e., the complete model).

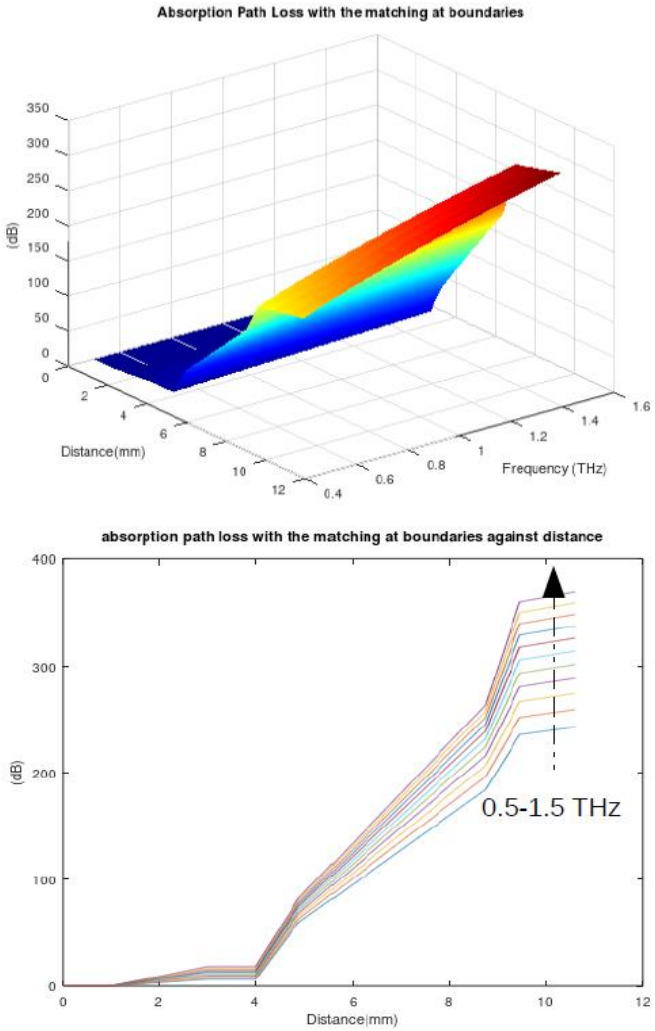

Figure 14. 3D and 2D absorption path-loss with boundary matching for the entire channel.

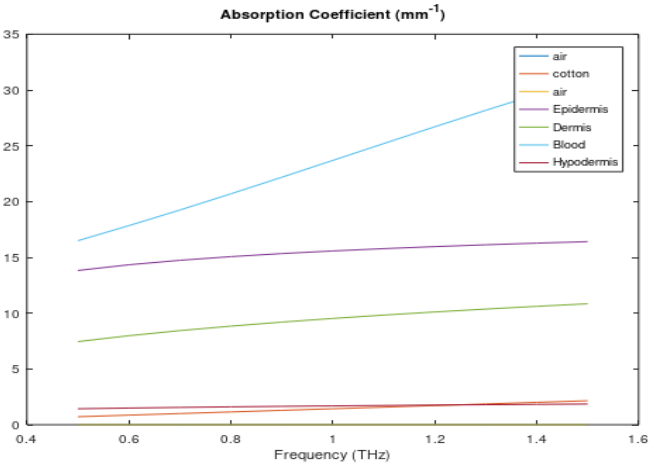

Figure 15. The frequency dependent absorption coefficient of the 7 layers in the entire channel.

Finally, the total path-loss is illustrated in Figure 16 for all the seven layers stacked together. We note that the total path-loss for an electromagnetic signal traveling through a stack of

depth 12 mm over a range of frequencies between 0.5 and 1.5 THz could be between 0 and 450 db.

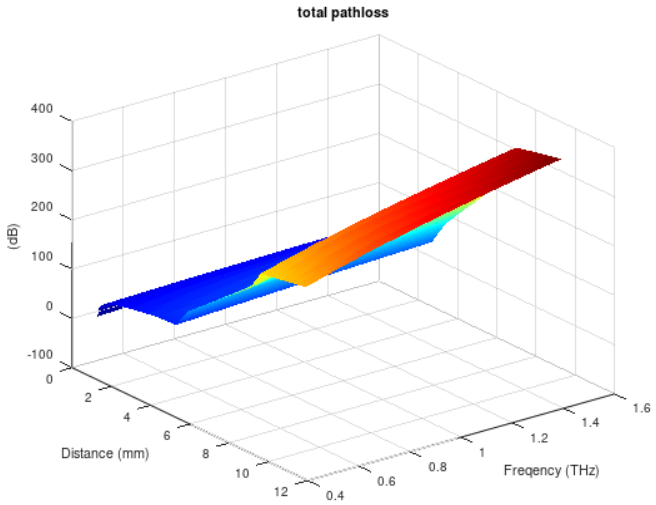

Figure 16. The total path-loss for the entire channel.

3.4 Reverse-way path-loss

The previous analysis takes care only of one direction of the communication from outside the human body to inside. For completeness, we did the same analysis of the path-losses in the other direction from inside to outside the human body. The results are shown in Figure 17, where we can notice that the total path-loss for an electromagnetic signal traveling through a stack of depth 12 mm over a range of frequencies between 0.5 and 1.5 THz could occur between 0 and 500 db. The loss at the end of the 12mm increases. The losses at the early stages in the direction from inside to outside is less than that from the other direction on the early distance.

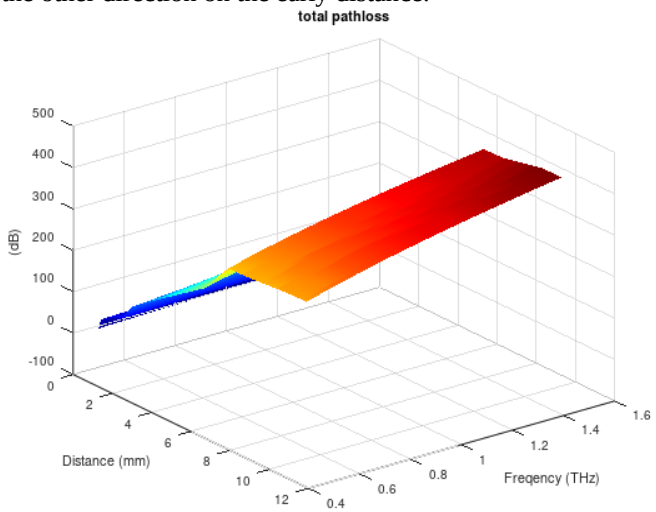

Figure 17. The total path-loss for the entire channel in the reverse direction (from inside to outside the human body).

4. Discussion

Results of the in-body model are very close to the results of [3], which validates this work implementation of the in-body model. Regarding the outside model, several related works are used, such as: explosive detection [11], impedance matching and multi-layer reflection. The main concern is to match the gap between the in-body and outside to be used in different applications.

In the considered frequency (0.5-1.5 THz), it is noticed that the absorption and delay are less sensitive to frequency. The reflections on the boundaries have a significant effect on the attenuation. The spreading path-loss does not seem to be very material dependent. In fact, it only differs by a few dB when tested on different materials over large distances.

It is worth noting that we have considered several simplifications in our current model. We have several ideas to further improve the model in the future work. Mainly, we can gradually add more sophistication to layer representation and layer number to better mimic the real world. For example, the skin has many other factors that may affect the model such as: blood, capillaries, hair follicles and sweat. Similarly, for the outside part that includes the textile layer, several influencing factors such as temperature, humidity or the composition and the form of the cotton fabrics could be taken into consideration. Especially that some previous research shows a significant effect of these factors on the THz signals [5], [17], [18]. Not only that, but we can also add a layer above or below the textile layer to study channel characterization when the patient applies some medical gel or ointments on the skin. The suggested future work could be feasible because we have already built our modelling software in a flexible manner to allow modifying the layer number, order and composition. This opens the possibility of adding more sophistication or considering new use cases that may arise in various applications.

5. Conclusion

A model for in-body-outside communication channel in THz band is developed. The model was progressively built in three steps: in-body model (human body), Outside (on-body) model (air-cotton-air) and after validating these models by comparing with results from previously published works, a fused model is created by combining both the in-body and outside models (human body-air-cotton-air). This model is implemented in Octave program to enable modifying the important properties such as layer type and thickness. We provide a study of the behavior of the THz signal being propagated through body tissues and outside layers. In particular, the analysis of spreading path-loss, the absorption path-loss and the reflection loss is performed over a range of terahertz frequencies from 0.5 to 1.5 THz.

Regarding the in-body sub-model, the spreading path-loss does not seem to be very material dependent with respect to human body tissues. In fact, it only differs by few dB when compared with different materials side by side over the whole distance. The absorption path-loss is higher than that of the spreading path-loss where we can observe clear differences between the different tissues. Regarding the on-body sub-model, the significant loss occurs when the signal traverses the cotton layer where it suffers from the highest amount of attenuation, which is expected when compared to the loss in the air layers (almost 0). However, in practice, the humidity, the temperature and the presence of water vapor particles would certainly affect the losses in the air layers. Our final goal is to study losses in the entire channel that consists of human body tissues and cotton layer. For completeness, we did the same analysis of the path-losses in the other direction from inside to outside the human body.

We have used mathematical equations to produce our results, which are then validated by comparison with previous reported work. In future work, we could use measurement

instruments such as time domain spectroscopy (TDS) to obtain more rigorous validation. Future improvements could also include calculating the channel capacity and delays for the entire channel, characterization of the model will be examined in different environmental conditions, using different type of textiles, adding a layer such as: paraffin wax for more realistic medical application. Furthermore, we could consider thread thickness and sewing patterns that may affect THz wave propagation and reflection through textiles.

References

[1] P. Garbacz, "Terahertz Imaging - Principles, Techniques, Benefits and Limitations," *Probl. Eksploat. - Maint. Probl.*, vol. 100, pp. 81–92, Jan. 2016.

[2] I. F. Akyildiz, J. M. Jornet, and C. Han, "Terahertz band: Next frontier for wireless communications," *Phys. Commun.*, vol. 12, pp. 16–32, Sep. 2014, doi: 10.1016/j.phycom.2014.01.006.

[3] C. Pettersson, "Modeling and Characterization of a Propagation Channel in a Body-Centric Nano-Network," p. 30.

[4] K. Yang, A. Pellegrini, M. O. Munoz, A. Brizzi, A. Alomainy, and Y. Hao, "Numerical Analysis and Characterization of THz Propagation Channel for Body-Centric Nano-Communications," *IEEE Trans. Terahertz Sci. Technol.*, vol. 5, no. 3, pp. 419–426, May 2015, doi: 10.1109/TTHZ.2015.2419823.

[5] J. Li and J. Li, "Optical characteristic of cotton in the THz frequency region," p. 6.

[6] N. Atanasov, G. Atanasova, and B. Atanasov, "Wearable Textile Antennas with High Body-Antenna Isolation: Design, Fabrication, and Characterization Aspects," in *Modern Printed-Circuit Antennas*, H. Al-Rizzo, Ed. IntechOpen, 2020. doi: 10.5772/intechopen.91143.

[7] S. Jaruwatanadilok, Y. Kuga, A. Ishimaru, and E. Thorsos, "An electromagnetic model for detecting explosives under obscuring layers," p. 10.

[8] John W. Eaton *et. al.*, "GNU Octave version 6.3.0 manual"., Accessed: Sept 07, 2021. [Avialble online]: http://www.gnu.org/software/octave/doc/interpreter/

[9] Mathworks inc, "Matlab Platform", Accessed: Sept. 7, 2021 [Available Online]: https://www.mathworks.com/products/matlab.html

[10] H. T. Friis, "A note on a simple transmission formula," Proc. IRE 34,254–256, 1946.

[11] D. F. Swinehart, "Beer–Lambert law", Journal of Chemical Education, vol. 39, issue 7, p. 333, July 1962. DOI: 10.1021/ed039p333.

[12] A. S. Volkov, G. D. Koposov, R. O. Perfil'ev, and A. V. Tyagunin, "Analysis of Experimental Results by the Havriliak–Negami Model in Dielectric Spectroscopy," *Opt. Spectrosc.*, vol. 124, no. 2, pp. 202–205, Feb. 2018, doi: 10.1134/S0030400X18020200.

[13] "Debye relaxation, Dielectric constant, Loss factor, Butan-1-ol and Ethanol," *Am. J. Condens. Matter Phys.*, p. 7, 2015.

[14] T. Igarashi, K. Nishino, and S. K. Nayar, "The Appearance of Human Skin: A Survey," *Found. Trends® Comput. Graph. Vis.*, vol. 3, no. 1, pp. 1–95, 2007, doi: 10.1561/0600000013.

[15] C. B. Reid, G. Reese, A. P. Gibson, and V. P. Wallace, "Terahertz Time-Domain Spectroscopy of Human Blood," *IEEE J. Biomed. Health Inform.*, vol. 17, no. 4, pp. 774–778, Jul. 2013, doi: 10.1109/JBHI.2013.2255306.

[16] D. Kurup, G. Vermeeren, E. Tanghe, W. Joseph, and L. Martens, "In-to-Out Body Antenna-Independent path-loss Model for Multilayered Tissues and Heterogeneous Medium," p. 15, 2015.

[17] H. Elayan, R. M. Shubair, J. M. Jornet, and P. Johari, "Terahertz Channel Model and Link Budget Analysis for Intrabody Nanoscale Communication," *IEEE Trans. NanoBioscience*, vol. 16, no. 6, pp. 491–503, Sep. 2017, doi: 10.1109/TNB.2017.2718967.

[18] Yusuke Mukai, "Dielectric Properties of Cotton Fabrics And Their Applications", PhD Thesis, North Carolina State University, 2019.

[19] A. Basnet, A. Alsadoon, P. W. C. Prasad, O. H. Alsadoon, L. Pham, and A. Elchouemi, "A Novel Secure Patient Data Transmission through Wireless Body Area Network: Health Tele- Monitoring," vol. 11, no. 1, p. 12, 2019.